Naturwissenschaften (2010) 97:1067–1076
DOI 10.1007/s00114-010-0728-1

ORIGINAL PAPER

Solar energy harvesting in the epicuticle of the oriental hornet (*Vespa orientalis*)

Marian Plotkin · Idan Hod · Arie Zaban · Stuart A. Boden · Darren M. Bagnall · Dmitry Galushko · David J. Bergman

Received: 28 September 2010 / Accepted: 11 October 2010 / Published online: 29 October 2010

Abstract The Oriental hornet worker correlates its digging activity with solar insolation. Solar radiation passes through the epicuticle, which exhibits a grating-like structure, and continues to pass through layers of the *exo*-endocuticle until it is absorbed by the pigment melanin in the brown-colored cuticle or xanthopterin in the yellow-colored cuticle. The correlation between digging activity and the ability of the cuticle to absorb part of the solar radiation implies that the Oriental hornet may harvest parts of the solar radiation. In this study, we explore this intriguing possibility by analyzing the biophysical properties of the cuticle. We use rigorous coupled wave analysis simulations to show that the cuticle surfaces are structured to reduced reflectance and act as diffraction gratings to trap light and increase the amount absorbed in the cuticle. A dye-sensitized solar cell (DSSC) was constructed in order to show the ability of xanthopterin to serve as a light-harvesting molecule.

Keywords Oriental hornet *Vespa orientalis* · Cuticle · Dye-sensitized solar cell · *I–V* measurements · Antireflection · Light trapping · Diffraction grating

M. Plotkin (✉)
Department of Physiology and Pharmacology,
Sackler Faculty of Medicine Tel-Aviv University,
Ramat Aviv 69978, Israel
e-mail: marianpl@post.tau.ac.il

I. Hod · A. Zaban
Institute of Nanotechnology and Advanced Materials,
Department of Chemistry, Bar Ilan University,
52900 Ramat Gan, Israel

S. A. Boden · D. M. Bagnall
Nano Research Group, Electronics and Computer Science,
University of Southampton,
Highfield,
Southampton SO17 1BJ, UK

D. Galushko
Department of Physics, Technion-Israel Institute of Technology,
Haifa 32000, Israel

D. J. Bergman
School of Physics and Astronomy, Raymond and Beverly Sackler
Faculty of Exact Sciences, Tel-Aviv University,
Ramat Aviv 69978, Israel

Introduction

The pattern of activity of several species of wasps have been studied (Gaul 1952; Potter 1964; Edwards 1968; Iwata 1976), and they all have shown a similar mode of behavioral pattern. The greatest period of activity is in the early morning when the wasps leaving and entering the nest are nearly twice as active as for the remainder of the day. The latter period of time is characterized by a fairly constant activity with a sudden drop in the evening. The Oriental hornet, in contrast, shows a peak of activity in the middle of the day (Ishay et al. 1967). The number of Oriental hornet workers emerging from the nest entrance around noon is by two orders of magnitude greater than the number of those emerging in the morning or evening hours.

The Oriental hornet is a social insect that exhibits intricate behavioral patterns (Spradbery 1973). It builds its nest underground, and to that aim, the worker hornet digs the soil and removes it from the nest repeatedly. It does so by picking up the soil in its mandibles and flying out of the nest for a short distance, dropping the soil in mid air, and returning to the nest to repeat this activity (Fig. 1a). The Oriental hornet correlates its digging activity with insolation: as insolation increases, the Oriental hornet increases its activity. and likewise, as insolation decreases, it decreases

digging activity (Ishay 2004). In a previous study (Volynchik et al. 2008), we were looking for a correlation between meteorological factors [i.e., temperature, humidity and ultraviolet B (UVB)] and diurnal hornet digging activity. The only significant correlation observed was between UVB radiation and hornet-digging activity. The complex structure of the cuticle is produced by extracellular secretion from the epidermis. It is constructed as a composite consisting of chitin filaments, structural proteins, lipids, catecholamine derivatives, and minerals. The Oriental hornet cuticle (the exoskeleton) exhibits a brown-yellow pattern which serves to warn potential predators that it is venomous (Fig. 1b). The process of pigment formation in the cuticle takes about 3 days post-eclosion to be completed. During this time, the Oriental hornet exhibits a photophobic reaction to light, hiding from sunlight if the nest is exposed. When pigment formation is completed, the hornet is ready to exit the nest (Plotkin et al. 2009a). The yellow segments protect the cuticle from potentially harmful solar UV radiation, similar to the role of melanin in the brown color segments of the hornet's body (Fig. 1c). The Oriental hornet epicuticle exhibits a terrace-like structure (Ishay et al. 2002). The brown cuticle is made up of about 30 layers, whose thickness diminishes from the exterior to the interior (Ishay et al. 1998), ranging from about l–2 μm in the outermost layer of the exocuticle down to about 30–50 nm in the innermost layer of the hypocuticle (Fig. 1d). The brown pigment melanin lies within those layers. The yellow cuticle is made up of about 15 layers of *exo*-cuticle–*endo*-cuticle beneath them, where lies the yellow pigment granules with an underside of a thin layer of hypo-cuticle (Ishay and Pertsis 2002; Fig. 1e). The yellow segments contain xanthopterin (Plotkin et al. 2009b), which is housed in an array of barrel-shaped granules (Fig. 1f). We demonstrated that certain liver-like functions are performed in the yellow pigment layer (Plotkin et al. 2009c). The enzymatic activity in the layer of yellow granules was higher in hornets kept in dark conditions and lower in hornets exposed to UV light. We have shown in a previous study (Plotkin et al. 2010) that measurement of the voltage between the hypocuticle and the exocuticle of the yellow stripe showed a negative potential at the hypocuticle with respect to the positive exocuticle. In response to illumination of the yellow stripe, the difference in potentials between light and darkness increases. Placement of the stripe in darkness caused a drop in the potential. Pterins have a role in photoreception and phototransduction of near-UV light to blue light. It has been suggested that pterins play some role in photosynthesis (Fuller et al. 1971) and may act as blue antennas in superior plants (Galland and Senger 1988). The fact that the Oriental hornet correlates its digging activity with insolation, coupled with the ability of its cuticular pigments to absorb part of the solar radiation, may suggest that some form of solar energy harvesting is performed in the cuticle. The aim of this article is to explore this intriguing possibility by exploring the morphology of the cuticle and its biophysical characterization.

Materials and methods

Atomic force microscopy

The second dorsal gastral segment (brown) and the third dorsal gastral segment (yellow) were measured by atomic force microscopy (AFM, Molecular Imaging Pico Plus) with the use of PicoScan5 software. Scanning was performed in tapping mode in air, using NSC35/AIBS noncontact silicon probes purchased from MikroMasch. Results were analysed with the use of WsXM 5 software (Horcas et al. 2007).

Preparation of slices of *exo*-endocuticle for ESEM

Dorsal cuticular segments were immersed in liquid nitrogen then fractured to reveal their internal structure. The third dorsal gastral segment was from an Oriental hornet worker 3 days pre-eclosion and from a cuticle 3 days post-eclosion (to compare between morphological changes and reflectivity). The segments were fixed at 4°C in 3% (V/V) glutaraldehyde in phosphate buffered saline (PBS) overnight. After several washings in PBS, the tissue was postfixed in 1% OsO_4 in PBS for 2 h. Dehydration was carried out in graded ethanol and embedding in glycid ether. Two micron sections were cut for observation. The cuticular sections were viewed via the Quanta 200 FEG environmental scanning electron microscope (ESEM). The samples were imaged with the secondary electron large-field detector [lateral force microscopy (LFM)] in low vacuum mode of 70 Pa as previously described (Plotkin et al. 2009a).

Reflectance

Reflectivity of cuticular stripes was measured on the double monochromator Lambda 900 UV/visible (VIS)/infrared (IR) spectrometer. The dual-channel scheme was used for conducting measurements: a front surface mirror with known reflectance was placed in a reference channel and samples were placed in a sample compartment. Measurements were conducted in a spectral range of 400–850 nm with a step of 1 nm. Measurement accuracy was about 1%.

Optical modeling

The brown and yellow cuticle surfaces were modeled using rigorous coupled wave analysis (RCWA), implemented using a commercial software package (GD-Calc.; Nevière

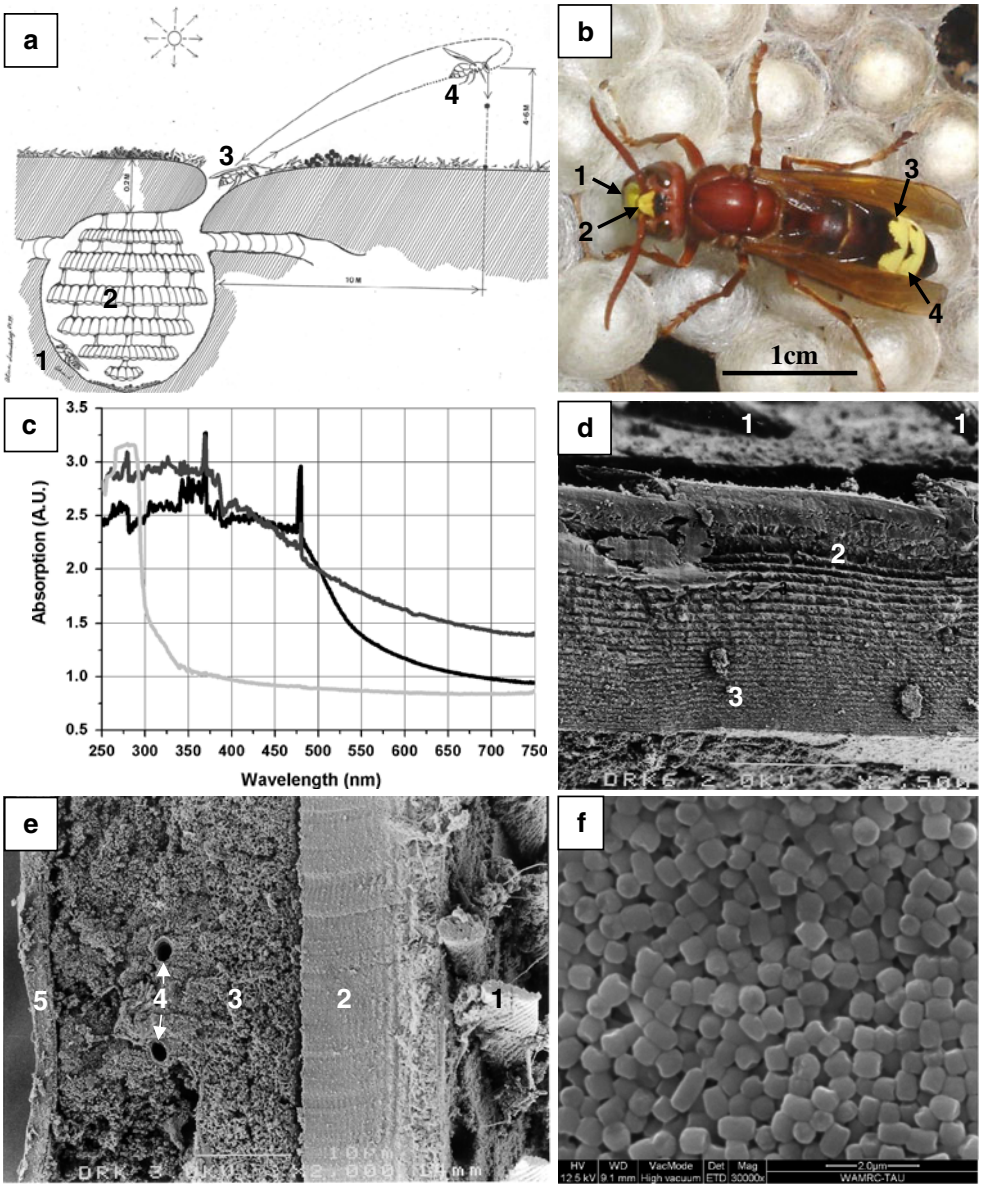

Fig. 1 Relationship between the Oriental hornet flight activity, exposure to solar radiation and the absorbance of this solar radiation in the cuticle. **a** Drawing represents the digging activity of the Oriental hornet worker. The Oriental hornet digs its nest (*1*) and enlarges it to allow for the building of additional comb cells (*2*). The hornet picks a clod of earth in its mandible (*3*), flies out of the nest, drops the clod of earth (*4*), and returns to repeat this process. **b** Picture showing an Oriental hornet resting on silk caps that harbor the pupae. The brown-colored hornet has yellow-colored segments on its head: the front (*1*), the clypeus (*2*), on the dorsal side of its abdomen, stripe nos. 3 and 4 (*3* and *4*), and one stripe on the ventral side of the abdomen (not shown in **b**). Bar=1 cm. **c** Graph represents typical results of cuticle absorbance obtained in an earlier study (Plotkin et al. 2009b). The graph displays the absorbance of brown cuticle, yellow cuticle, and yellow cuticle after the removal of yellow pigment granules. The brown and yellow cuticles display similar characteristics with absorbance highest at the shorter wavelengths. Absorbance in the range of 250–290 nm after the removal of pigment granules is attributed to the aromatic amino acids which constitute the proteins present in the hornet cuticle (Willis 1999). **d** Cross-section through the cuticle of an adult hornet brown cuticle. Shown are the hairs extruding from the exocuticle (*1*), the cuticle is made up of about 30 layers whose thickness diminishes from the exterior (*2*) to the interior (*3*). **e** Cross-section through the cuticle of an adult hornet containing yellow granules. Shown are the hairs extruding from the exocuticle (*1*); the exocuticle proper and the endocuticle (*2*), and beneath the latter, the layer of yellow granules (*3*), within the layer of yellow granules, tracheae are discernible (*4*), and underneath the hypocuticle (*5*). Bar=10 μm. **f** On greater magnification, one can see the barrel-like shape of the yellow pigment granules (about 500 nm in size) and that they are tightly packed. Bar=2 μm

and Popov 2003; Johnson 2008). The surface structures of the two types of cuticle were recreated in GD-Calc using a staircase approximation, with 30 strata. The optical properties of the multilayer structure below the surface of the epicuticle are as yet unknown and so the full structure could not be modeled. We decided to concentrate on the effects that the top surface topography has on the incident light so in order to isolate these effects, a homogeneous substrate was used, rather than a multilayer. The refractive index of the epicuticle surface features and the homogeneous substrate was defined as 1.56 (i.e., of chitin). The medium above the epicuticle surface was defined with a refractive index of 1 (i.e., of air). GD-Calc was then used to calculate the diffraction efficiencies of each reflected order for transverse electric (TE or s) and transverse magnetic (TM or p) polarizations, for light incident normal to the surface, over a wavelength range from 400 to 850 nm, with an interval size of 5 nm. The maximum number of diffraction orders included in the calculations was 10, by which point convergence tests demonstrated that the solutions had converged. The diffraction efficiencies were summed to give a total reflectance for each wavelength, thus allowing the generation of reflectance versus wavelength plots and the antireflection (AR) properties of surface structure to be investigated.

Another possible optical role for the observed surface textures is that of diffraction gratings which would cause light passing through the surface to be distributed between the zero-order specular beam, traveling normal to the surface, and several higher orders that propagate at other angles relative to the normal. These orders will travel through more cuticle material per pass and may undergo total internal reflection at the back surface. Thus, redirection back through the layers will result in a higher absorption. This phenomenon, known as light trapping, would act in addition to any AR effect to cause more light to be absorbed than if the surface was flat. RCWA was used to probe the diffraction properties of the brown epicuticle structure, which resembles a classic grating design. By treating the brown epicuticle as a 20 μm homogenous layer of chitin containing melanin pigment (i.e., neglecting effect of the internal layered structure seen in Fig. 1d), we can assess the amount of extra light absorbed as a result of the grating structure conferring an antireflective and light-trapping effect compared to if the surface was flat. For a flat surface, only the specularly transmitted beam is present and so the intensity of light remaining after one pass through the epicuticle, $I_f(\lambda)$, is given by:

$$I_f(\lambda) = I_{0f}(\lambda)e^{-\alpha(\lambda)t}$$

where $I_{0f}(\lambda)$ is the intensity of light transmitted by the flat surface (i.e., 1-reflectance), t is the thickness of the epicuticle layer, and $\alpha(\lambda)$ is its absorbtion coefficient. The fraction of incident light absorbed in the flat epicuticle (absorptance, A_f) after one pass is then given by:

$$A_f = 1 - R_f(\lambda) - I_f(\lambda)$$

where $R_f(\lambda)$ is the total reflectance of the surface.

Since the concentration of melanin in the brown epicuticle is unknown, an empirical fit to experimental data for absorption in human skin was used as a reasonable first approximation of the absorption properties of the brown epicuticle. The absorption coefficient of melanin in human skin in cm^{-1}, $a_{cm}{}^{-1}$, as a function of wavelength in nm, λ_{nm}, is given by (Jacques 1998):

$$\alpha_{cm^{-1}}(\lambda) = 1.70 \times 10^{12}\lambda_{nm}^{-3.48}$$

The grating structure introduces 1 and −1 transmitted orders for λ>752 nm, propagating at an angle $\theta(\lambda)$, with intensities $I_{1g}(\lambda)$ and $I_{-1g}(\lambda)$, respectively, as well as the zero-order transmitted beam of intensity I_{0g}. The 1 and −1 orders travel through a thickness t', where

$$t'(\lambda) = \frac{t}{\cos\theta(\lambda)}$$

The total remaining intensity after one pass through the brown epicuticle with the grating structure surface, $I_g(\lambda)$, is given by summing the contributions from the 1, 0, and −1 orders:

$$I_g(\lambda) = I_{0g}(\lambda)e^{-\alpha(\lambda)t} + [I_{1g}(\lambda) + I_{-1g}(\lambda)]e^{-\alpha(\lambda)t'(\lambda)}$$

The fraction of incident light absorbed in the epicuticle (absorptance, A_g) with the grating structure surface after one pass is then given by:

$$A_g = 1 - R_g(\lambda) - I_g(\lambda)$$

where $R_g(\lambda)$ is the reflectance of the grating.

DSSC construction

To test the hypothesis that xanthopterin can act as an absorber material for solar radiation, a dye-sensitized solar cell (DSSC, O'Regan and Grätzel 1991) was constructed using the following method:

Mesoporous TiO_2 films (12-μm-thick) were prepared by electrophoretic deposition (EPD; Grinis et al. 2008) of Degussa P25 particles with an average diameter of 25 nm onto fluorine-doped tin oxide (FTO) covered glass substrates (Pilkington TEC 15) with 15 Ω/square sheet resistances.

Films were deposited in four consecutive cycles of 60 s at a constant current density of 0.4 mA/cm^2 (which corresponded to 70 V at an electrode distance of 50 mm), and dried at 120°C for 5 min in between cycles. Following the EPD process, all the electrodes were dried in air at 150°C for 30 min, pressed under 800 kg/cm^2 using a hydraulic press,

and sintered at 550°C for 1 h. The thickness of the mesoporous electrodes was measured with a profilometer (Surftest SV 500, Mitutoye). The electrodes were subsequently immersed in 1 mM of xanthopterin in ethanol for 24 h and then rinsed with ethanol. An I-/I3-redox electrolyte was used in the xanthopterin-sensitized solar cell, consisting of 0.1 M lithium iodide, 0.05 M iodine, 0.6 M 1-propyl-2,3 dimethylimidazolium iodide, and 0.5 M 4-tertbutylpyridine dissolved in a solution of acetonitrile and 3-methoxypropionitrile at a ratio of 1:1. A Pt-coated FTO glass was used as a counterelectrode. Photocurrent–voltage characteristics were performed with an Eco-Chemie Potentiostat using a scan rate of 10 mV/s. A 250 W xenon arc lamp (Oriel) calibrated to 100 mW/cm^2 (AM 1.5 spectrum) served as a light source. The illuminated area of the cell was 0.64 cm^2.

DSSCs provide a technically and economically credible alternative concept to crystalline silicon-based p–n junction photovoltaic devices. In contrast to conventional systems, where light absorption and charge carrier transport takes place in the semiconductor, these two processes are separated in DSSCs. Light is absorbed by a sensitizer which is anchored to the surface of a mesoporous wide band gap semiconductor film (usually TiO_2). Charge separation takes place at the dye/semiconductor interface via a two-step photo-induced process. First, an electron is excited from the HOMO to the LUMO level of the dye, followed by injection into the conduction band of the semiconductor. After charge separation, electrons diffuse through the mesoporous semiconductor toward a conducting transparent front electrode, while positive charges are transported by the electrolytes' redox species to a Pt back electrode.

Results

Two distinct patterns emerge from the AFM study. The Oriental hornet's brown cuticle surface consists of an array of grooves with a height of about 160 nm and a period of about 500 nm (Fig. 2a, b). The Oriental hornet's yellow cuticle shows small protrusions, oval in shape, with one or two "pinhole" depressions at every protrusion. The protrusions exhibit an interlocking pattern. Its height is about 50 nm with a period of about 500 nm (Fig. 2c, d). Fracturing the cuticle following immersion in liquid nitrogen reveals its layered configuration (Fig. 3a). Each layer is made of chitin fibers immersed in protein matrix (Fig. 3b). *Exo*-endocuticle formation process is completed 3 days post-eclosion. The fixation process of this fully formed cuticle reveals that between one layer and the next, there is a thin plate. Those plates are arranged in a parallel configuration with short pillar-like structures that separate one plate from the other (Fig. 3c). The thickness of each plate is 158±32 nm (mean±SD) and the thickness of each pillar is 70±17 nm (mean±SD). Looking at a cuticle of a pupa 6 days earlier, i.e., 3 days pre-eclosion, reveals a disorganized structure (Fig. 3d). The organized parallel plated structure of an adult hornet has not yet been formed. Reflectivity measurements showed that within a measured region of 400–850 nm, the cuticle exhibited similar characteristics in all the samples measured (Fig. 4). Within a region of 400–600 nm, the cuticle displayed stable low reflectivity, which started to increase toward the IR. Reflectivity of both the brown and yellow cuticles was lower in the mature cuticle (3 days post-eclosion) compared to that of pupal cuticles (3 days pre-eclosion). The reflectivity of the brown and yellow cuticles exhibited similar properties except in the 700–850 nm region, where the brown cuticle displayed greater reflectivity than the yellow cuticle. This is attributed to the pigment properties in each segment. The surface structure of the cuticle was created in GD-Calc (Fig. 5a, c). The modeled reflectance versus wavelength plot for the brown epicuticle surface structures (Fig. 5b) shows that the ridge/groove structure confers an antireflective effect, with the average reflectance across the wavelength range decreasing by 54% from 0.048 to 0.022 when compared with a flat chitin surface. The corresponding plot for the yellow cuticle (Fig. 5d) suggests that this structure confers a much weaker antireflective effect that the brown cuticle surface, with an average reflectance across the wavelength range, is decreased by only 8.3% from 0.048 to 0.044, as compared to a flat surface. Results of the analysis of the brown epicuticle surface structures as diffraction gratings are presented in Fig. 6. Only the zero order propagates in transmission for $\lambda > nd$, where λ is the wavelength, d is the grating period, and n is the refractive index of the grating substrate. For the brown epicuticle, this is the case for $\lambda > 752$ nm. For wavelengths less than 752 nm, the 1 and −1 orders also propagate in transmission, with an angle relative to normal that decreases with decreasing wavelength (Fig. 6d). The efficiencies of the 0, 1, and −1 orders for TE, TM, and the average of TE and TM polarizations are plotted as a function of wavelength in Fig. 6a–c. The proportion of light absorbed (absorptance, A_g) in one pass through a 20-μm-thick brown epicuticle layer with the grating surface, as a function of wavelength, is compared to the absorptance, A_f, if the surface was flat (Fig. 6e). The antireflective and light-trapping properties conferred by the grating structure lead to a 5.1% increase in absorptance from 0.489 to 0.514, averaged across the wavelength range. In order to show that xanthopterin can act as an absorber material for a photovoltaic device, a DSSC was constructed using xanthopterin as the dye molecule. Characterization of the performance of xanthopterin-sensitized solar cell was done using *I–V* measurements (Fig. 7), which exhibit an open-circuit voltage of 564 mV, a short-circuit current of 0.858 mA/cm^2, and a fill factor of 69.2%, resulting in a conversion efficiency of 0.335%.

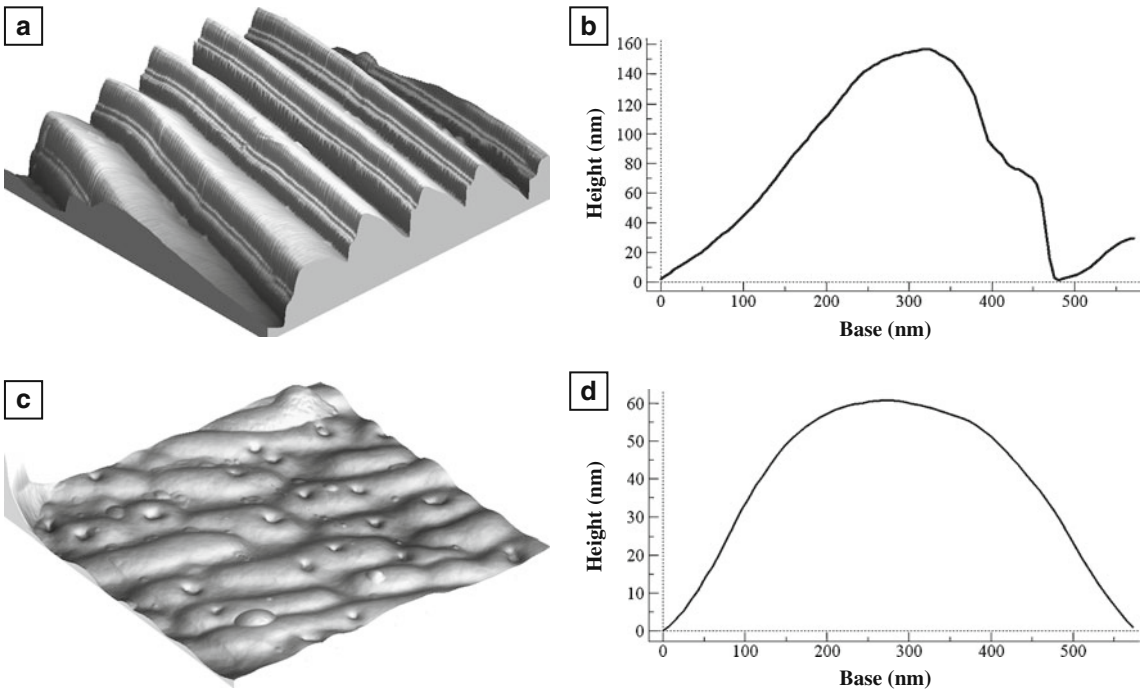

Fig. 2 Findings from the AFM study of the brown and yellow epicuticle (cuticle surface). **a** 3D image of the brown cuticle, showing the grating structure. **b** The profile structure of the grating on the brown cuticle. The grating-like formation has a height of about 160 nm and a period of about 500 nm. **c** 3D image of the yellow cuticle showing the interlocking pattern of oval-shaped structures. Every oval structure harbors at least one "pinhole" depression. **d** The profile structure of the grating on the yellow cuticle

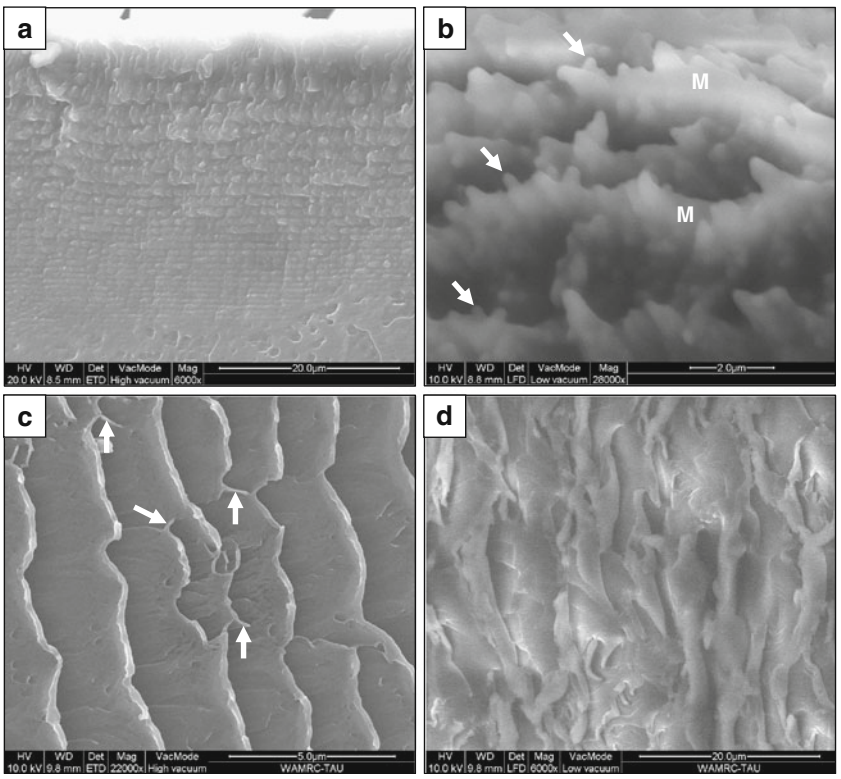

Fig. 3 Oriental hornet's *exo*-endocuticle structure. **a** Fractured cuticle after immersion in liquid nitrogen reveals the internal cuticular structure. The cuticle is made up of layers with thickness that diminishes from the exterior to the interior. **b** Magnification of a fractured section after immersion in liquid nitrogen reveals the chitin fibers (see *arrows*) within every layer, embedded in a protein matrix (*M*). **c** Fixation process reveals that, in the adult hornet cuticle (3 days post-eclosion), there are thin plates that separate one cuticular layer from the next; the structure is arranged in parallel plates, with short pillar-like structures that separate one plate from another (see *arrows*). **d** Fixation process reveals that, in pupa (3 days pre-eclosion), the structure is disorganized. The organized parallel plated structure of an adult hornet has not yet been formed

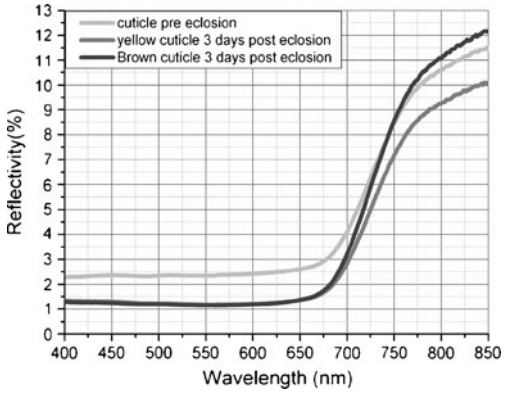

Fig. 4 Measured reflectivity of the hornet cuticle: (1) cuticle pre-eclosion (2) yellow cuticle 3 days post-eclosion, (3) brown cuticle 3 days post-eclosion

Discussion

We have shown through RCWA simulations that the epicuticle acts as an antireflective layer. As a comparison, nipple arrays, such as those found on the eyes and wings of some species of moth, confer also an antireflective effect (Bernhard 1967; Parker 2000; Vukusic and Sambles 2003). With periods of ~200 nm, the moth-eye structures are on a scale below the wavelength range of solar radiation, which means they act as an effective medium, with an effective refractive index that changes gradually across the interface. With periods of ~500 nm, the structures on the brown and yellow epicuticles are not subwavelength across the solar spectrum and so do not act as a true effective medium in the same way as the moth-eye structures. Therefore, although conferring some antireflective effect, the surface structures observed on the Oriental hornet cuticles are far from optimized for this purpose. However, unlike the moth-eye arrays, which are too small to diffract light, the brown cuticle structure also acts as a diffraction grating, enhancing light trapping and so absorption within the cuticle. The 5.1% increase in absorption calculated for the brown epicuticle structure compared to a flat surface is likely to be an underestimate because it only accounts for one pass through the cuticle; the 1 and −1 orders are travelling at higher angles and so more of the light will undergo internal reflection at the back surface and pass through the cuticle a second time, resulting in even more absorption compared to a flat surface. These findings suggest the possibility that the surface structure has evolved to confer both AR and light-trapping properties to the epicuticle, enhancing the absorp-

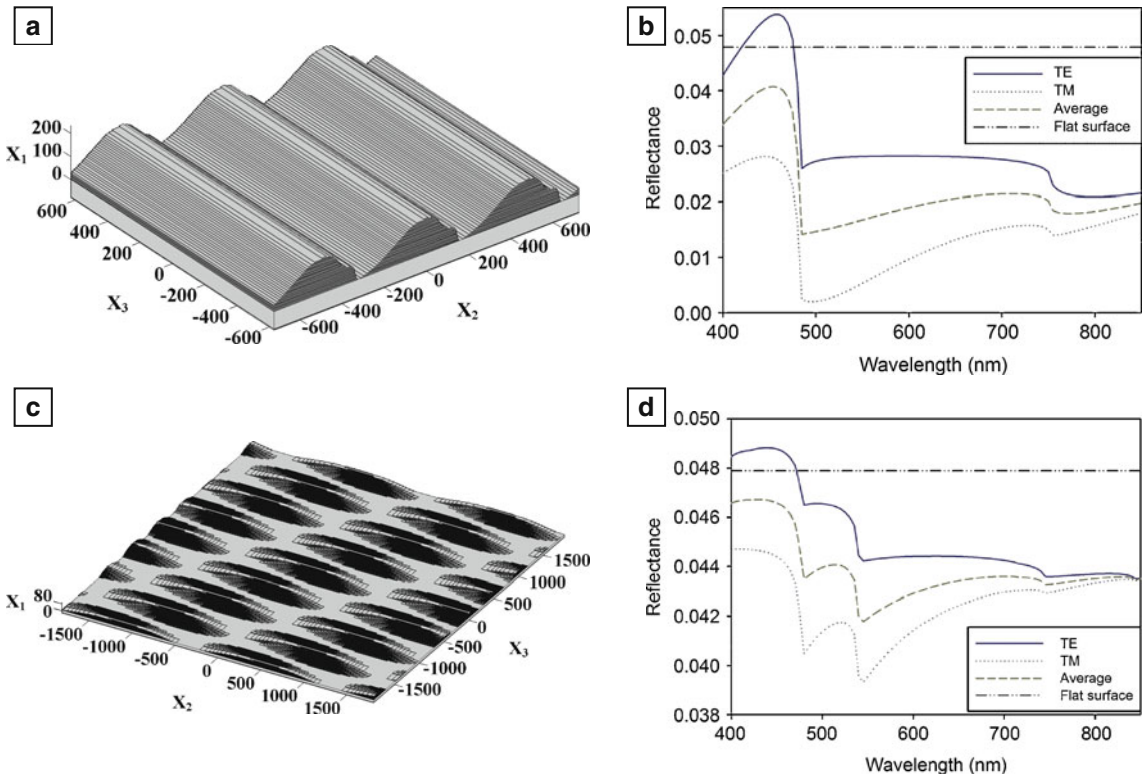

Fig. 5 Calculated reflectivity of the hornet cuticle surface. **a** Schematic of brown epicuticle defined in GD-Calc with 30 strata. The *grey* area shows material with a refractive index of $n=1.56$ (i.e., of chitin). The semi-infinite substrate is defined with $n=1.56$, and the semi-infinite superstrate medium is defined as air ($n=1$). **b** Reflectance vs. wavelength RCWA simulation for structure in (**a**). **c** Schematic of yellow epicuticle defined in GD-Calc with 30 strata The *grey* area shows material with a refractive index of $n=1.56$ (i.e., of chitin) The semi-infinite substrate is defined with $n=1.56$ and the semi-infinite superstrate medium is defined as air ($n=1$). **d** Reflectance vs. wavelength RCWA simulation for structure in **c**

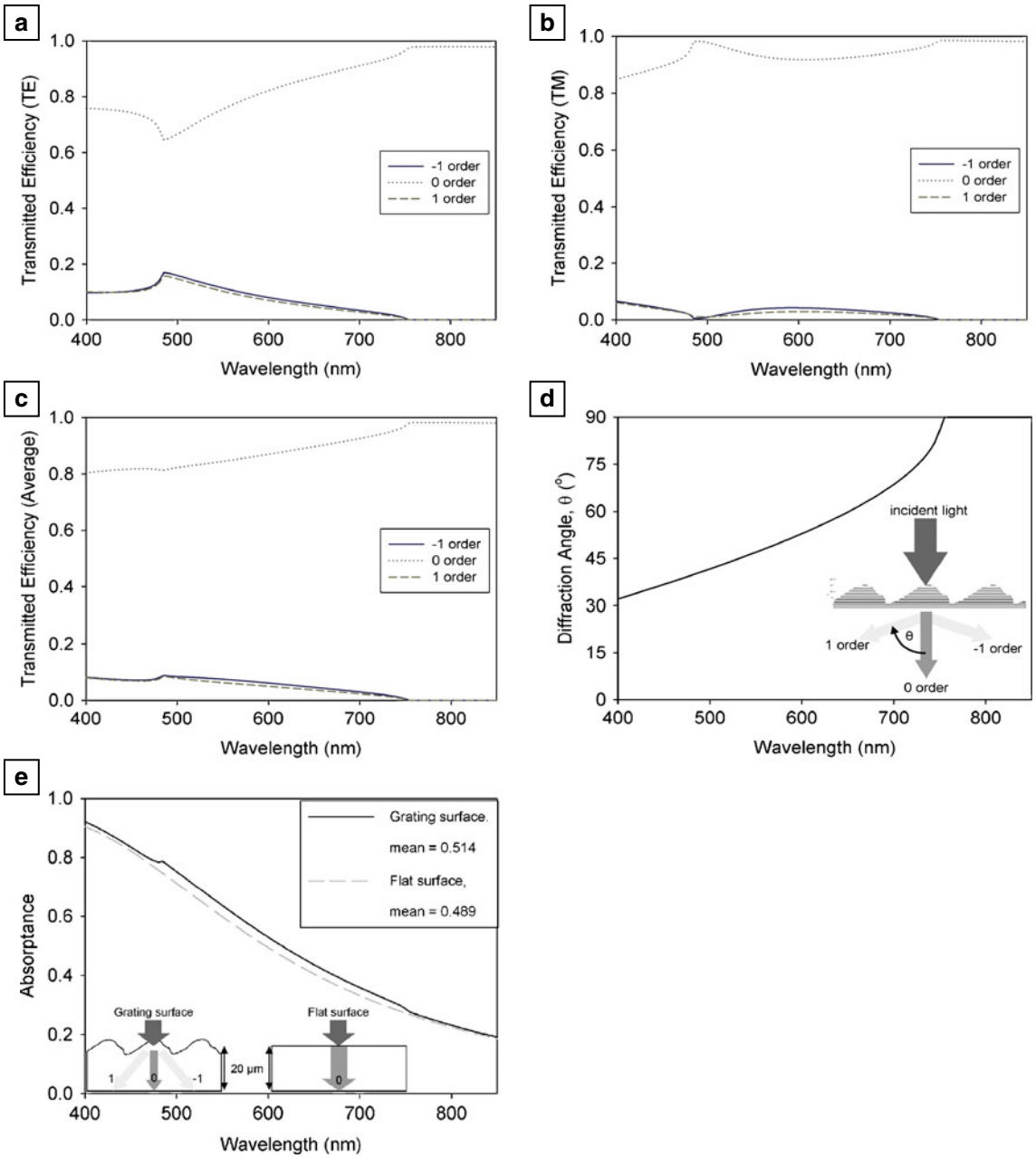

Fig. 6 Shows results from RCWA simulations of the brown epicuticle as a diffraction grating in transmission. **a** Calculated efficiencies of the transmitted 0, 1, and −1 orders as a function of wavelength for TE-polarized light at normal incidence on the brown epicuticle. **b** Calculated efficiencies of the transmitted 0, 1, and −1 orders as a function of wavelength for TM-polarized light at normal incidence on the brown epicuticle. **c** Calculated efficiencies of the transmitted 0, 1, and −1 orders as a function of wavelength for the average of TE- and TM-polarized light at normal incidence on the brown epicuticle. **d** Calculated variation with wavelength of the angle of the diffracted 1 and −1 orders with respect to the zero-order specularly transmitted beam for light at normal incidence on the simulated brown epicuticle surface. **e** Calculated absorptance (taken as an average of TE and TM polarizations) for a 20-μm-thick brown epicuticle with and without the grating structure found on the specimen, neglecting reflections from the back surface

tion of light within the cuticle of the hornet, resulting in more efficient collection of solar energy. Results of the optical modeling do not match the measured reflectance because they do not take into account the underlying layered structure; instead, it is assumed that the surface structure is formed in a semi-infinite chitin substrate. The Oriental hornet *exo*-endocuticle comprises a series of thin sheet-like structures, stacked on top of each other, with decreasing thickness from top to bottom (Fig. 3a). In every layer, there is circular rod-like structure composed of chitin chains packed together (Fig. 3b, arrows). The rods of chitin are embedded in a protein matrix (Giraud-Guille and

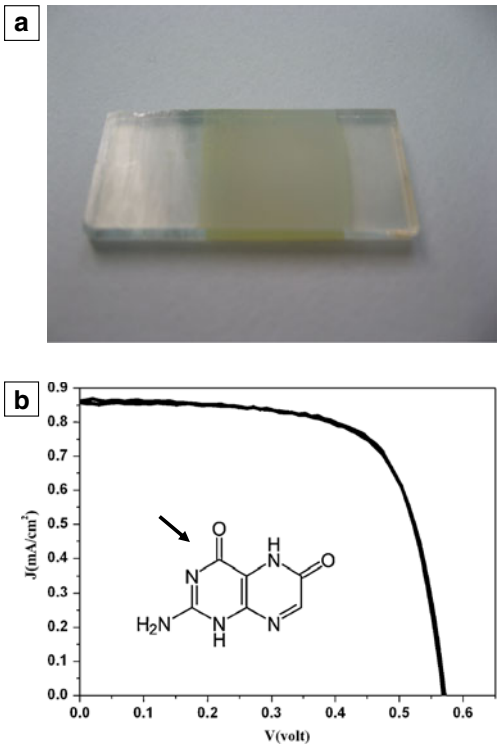

Fig. 7 Structure and performance of a xanthopterin-sensitized solar cell. **a** Image of a mesoporous TiO_2 electrode after immersion in a xanthopterin solution. **b** The *I–V* characteristics of a xanthopterin (see *arrow*)-sensitized solar cell under illumination

Bouligand 1986; Fig. 3b, M). The large differences between the measured (Fig. 4) and simulated (Fig. 5) reflectance results demonstrate that this underlying layered structure contributes to the overall reflectance properties of the epicuticle. The effective refractive index of the chitin rods and the protein matrix combined in each layer of the Oriental hornet cuticle is still unknown. The orientation of the rods in each layer and the impact of this orientation on the refractive index in each layer are still unclear, those questions will be elucidated in future studies. It is possible that the underlying layered structure introduces a gradual change in effective refractive index by varying the proportion of chitin and protein in each layer. Such an approach has been used by solar cell designers who have formed layers of nanorods, whereby the refractive index is controlled by changing the portion of air in each layer or by altering the angle of deposition of the nanorods (Chhajed et al. 2008; Kuo et al. 2008). Additionally, the Oriental hornet oval body structure means that the solar angle of incidence changes along its body, which may impact on the amount of light reflected. This problem could have been solved by the hornet by utilizing what may be an omnidirectional antireflective structure. Light passing through the yellow stripes is absorbed by xanthopterin, which serves as a light-harvesting molecule. The xanthopterin resides in tightly packed yellow pigment granules, which may serve to increase the effective surface area available for light absorption. Pterins are found in high concentrations in pierid butterflies (Wijnen et al. 2007). Pterins are housed in similar granular formation (beads) which allow absorption in the UV wavelengths while allowing an increase in the reflectance of higher wavelengths (Stavenga et al. 2004). The ability of xanthopterin to serve as a visible light absorber in a photo electrochemical solar cell is clearly evident from the *I–V* characteristics of the xanthopterin-sensitized solar cell. Previous studies have shown diffusion potential across the cuticle, with the inside negative with respect to the outside. Digby (1965) has suggested that electrons move through the semiconductive cuticular layer. This process creates calcium carbonate that precipitates in the cuticle. In conclusion, we have presented evidence supporting the hypothesis that the Oriental hornet has evolved a cuticle design to harvest solar energy. RCWA simulations show that the surface structures confer AR and light-trapping properties, enhancing absorption by approximately 5% compared to a flat surface. The xanthopterin pigment found within the cuticle has been proven to be a suitable absorber of light for the harvesting of solar energy by a demonstration of its use in an organic solar cell, with a conversion efficiency of 0.335%. Future work will focus in investigating the complex layered structure observed in the cuticle cross-sections, and its possible role in solar energy harvesting.

Acknowledgements The authors would like to thank the Bio-AFM Laboratory Manager, Dr. Artium Khatchatouriants, from the Center for Nanoscience and Nanotechnology at Tel Aviv University for his help and advice. We would like to thank Dr. Vered Holdengreber from the Electron Microscopy Unit, IDRFU Life Sciences at Tel-Aviv University for her help in the preparation of the cuticular slices of the *exo*-endocutile for ESEM analysis. This work was performed in partial fulfillment of the requirements for a PhD degree of Marian Plotkin.

Conflicts of interest None

References

Bernhard CG (1967) Structural and functional adaptation in a visual system. Endeavour 26:79–84

Chhajed S, Schubert MF, Kim JK, Schubert EF (2008) Nanostructured multilayer graded-index antireflection coating for Si solar cells with broadband and omnidirectional characteristics. Appl Phys Lett 93:251108

Digby PSB (1965) Semi-conduction and electrode processes in biological material I. crustacea and certain soft-bodied forms. Proc R Soc Lond B 161:504–525

Edwards R (1968) Some experiments on the rhythmic behaviour of the wasp *Vespula rufa* L. (Hymenoptera: Vespidae). MSc thesis. Univ. London

Fuller RC, Kidder GW, Nugent NA, Dewey VC, Rigopoulos N (1971) The association and activities of pteridines in photosynthetic systems. Photochem Photobiol 14:359–371

Galland P, Senger H (1988) The role of pterins in the photoreception and metabolism of plants. Photochem Photobiol 48:811–820

Gaul AT (1952) The awakening and diurnal flight activities of vespine wasps. Proc R Entomol Soc Lond A 27:33–38

Giraud-Guille MM, Bouligand Y (1986) Chitin-protein molecular organization in arthropods. In: Muzzarelli RAA, Jeuniaux Ch, Gooday GW (eds) Chitin in nature and technology. Plenum, New York, pp 29–35

Grinis L, Dor S, Ofir A, Zaban A (2008) Electrophoretic deposition and compression of titania nanoparticle films for dye-sensitized solar cells. J Photochem Photobiol A 198:52–59

Horcas I, Fernandez R, Gomez-Rodriguez JM, Colchero J, Gomez-Herrero J, Baro AM (2007) WSxM: a software for scanning probe microscopy and a tool for nanotechnology. Rev Sci Instrum 78:013705-1–013705-8

Ishay JS (2004) Hornet flight is generated by sunlight energy: U.V. irradiation counteracts anesthetic effects. J Electron Microsc 53:623–633

Ishay JS, Pertsis V (2002) The specific heat of the cuticle and the morphological difference between the brown and yellow cuticle of hornets. J Electron Microsc 51:401–411

Ishay J, Bytinski-Saltz H, Shulov A (1967) Contributions to the bionomics of the Oriental hornet *Vespa orientalis*. Israel J Entomol II:45–106

Ishay JS, Kirshboim S, Steinberg D, Kalicharan D, Jongebloed WL (1998) Hornet cuticle: a composite structure comprised of a series of duplex lamellae attenuating toward the interior of the body. Comp Biochem Physiol A 120:661–670

Ishay JS, Litinetsky L, Pertsis V, Barkay Z, Ben-Jacob E (2002) Sub-Micromorphology of the epicuticle of hornets: AFM studies. J Electron Microsc 51:79–86

Iwata K (1976) Evolution of instinct. Comparative ethology of hymenoptera. Translated from Japanese, 1971st edn. Amerind Publishing, New Delhi, pp 324–341

Jacques SL (1998) Melanosome absorption coefficient. http://omlc.ogi.edu/spectra/melanin/mua.html

Johnson KC (2008) GD-Calc- grating diffraction calculator. http://www.software.kjinnovation.com/GD-Calc.html

Kuo ML, Poxson DJ, Kim YS, Mont FW, Kim JK, Schubert EF, Lin SY (2008) Realization of a near-perfect antireflection coating for silicon solar energy utilization. Opt Lett 33:2527–2529

Nevière M, Popov E (2003) Light propagation in periodic media: differential theory and design. Marcel Dekker, New York

O'Regan B, Grätzel M (1991) A low-cost, high-efficiency solar cell based on dye-sensitized colloidal TiO_2 films. Nature 353:737–740

Parker AR (2000) 515 million years of structural colour. J Opt A Pure Appl Opt 2:R15–R28

Plotkin M, Volynchik S, Barkay Z, Bergman DJ, Ishay JS (2009a) Micromorphology and maturation of the yellow granules in the hornet gastral cuticle. Zool Res 30:65–73

Plotkin M, Volynchik S, Ermakov NY, Benyamini A, Boiko Y, Bergman DJ, Ishay JS (2009b) Xanthopterin in the Oriental hornet (*Vespa orientalis*): Light absorbance is increased with maturation of yellow pigment granules. Photochem Photobiol 85:955–961

Plotkin M, Volynchik S, Itzhaky D, Lis M, Bergman DJ, Ishay JS (2009c) Some liver functions in the Oriental hornet (*Vespa orientalis*) are performed in its cuticle: exposure to UV light influences these activities. Comp Biochem Physiol A 153:131–135

Plotkin M, Volynchik S, Hiller R, Bergman DJ, Ishay JS (2010) The Oriental hornet Vespa orientalis (Hymenoptera: Vespinae) cuticular yellow stripe as an organic solar cell: a hypothesis. In: Collignon LN, Normand CB (eds) Photobiology: principles, applications and effects. Nova, New York

Potter NB (1964) A study of the biology of the common wasp, *Vespula vulgaris*, L., with special reference to the foraging behaviour. PhD Thesis, Bristol University

Spradbery JP (1973) Wasps: an account of the biology and natural history of solitary and social wasps. Sidgwick and Jackson, London

Stavenga DG, Stowe S, Siebke K, Zeil J, Arikawa K (2004) Butterfly wing colours: scale beads make white pierid wings brighter. Proc R Soc Lond B 271:1577–1584

Volynchik S, Plotkin M, Bergman DJ, Ishay JS (2008) Hornet flight activity and its correlation with UVB radiation, temperature and relative humidity. Photochem Photobiol 84:81–85

Vukusic P, Sambles JR (2003) Photonic structures in biology. Nature 424:852–855

Wijnen B, Leertouwer HL, Stavenga DG (2007) Colors and pterin pigmentation of pierid butterfly wings. J Insect Physiol 53:1206–1217

Willis JH (1999) Cuticular proteins in insects and crustaceans. Am Zool 39:600–609